Canadian Conference - Pacific Conference on Earthquake Engineering 2023
Vancouver, British Columbia
June 25th – June 30th, 2023

Steel Double-Headed Stud Reinforcement in Beam-Column Joints for Seismic Resistance

Hatem Ibrahim[1] and Mamdouh El-Badry[2*]

[1]Associate Professor, Department of Structural Engineering, Cairo University, Giza, Egypt
[2]Professor, Department of Civil Engineering, University of Calgary, Calgary, AB, Canada
[*]melbadry@ucalgary.ca (Corresponding Author)

ABSTRACT

Current ACI and CSA code provisions for seismic design require reinforcing beam-column joints with closed hoops and crossties for confinement of the concrete core. In exterior and roof beam-column joints, the closed hoops and crossties, as well as the bends required for anchoring the beam bars, cause significant congestion in the joint. Double-headed studs are proposed as shear reinforcement in lieu of conventional hoops and crossties. Six full-scale beam-column joint specimens were tested under cyclic loading. Joints of four of the specimens were reinforced with double-headed studs of different arrangements and amounts. The remaining two specimens were used as control: one with a shear-deficient joint not provided with transverse reinforcement, and one with the joint reinforced with hoops and crossties as per the code requirements. The tests demonstrated that use of double-headed studs in place of hoops and crossties is a promising solution for steel congestion. The stud-reinforced joints exhibited satisfactory performance similar to the joint reinforced with standard hoops and crossties and considerably enhanced behavior in comparison with the shear-deficient joint.

Keywords: Beam-column joint, cyclic loading, double-headed studs, energy dissipation, stiffness degradation.

INTRODUCTION

In many earthquakes worldwide, reinforced concrete beam-column joints, particularly exterior ones, have been repeatedly identified as critical elements which fail prematurely, forming weak links in framed structures. Poorly detailed joints frequently fail either by diagonal tension cracking resulting from high shear forces when insufficient or no shear reinforcement is provided, or by pullout of the beam longitudinal bars before the joint reaches its full capacity, when their anchorage within the joint is not adequate [1]. Therefore, recent design codes require that beam-column joints be provided with closed hoops (stirrups), and crossties, as shear reinforcement and for confinement of the joint concrete core. The codes also require that the beam flexural reinforcement be extended inside the joint with sufficient anchorage length. The legs of the hoops and the crossties are anchored to the concrete by hooks or bends. The beam reinforcing bars are bent at 90 degrees at the end of the joint to achieve proper anchorage. The hooks and bends, and the necessary overlaps within the joint, lead to reinforcement congestion, causing construction difficulties, hence, increase in labor cost, and to reduction in the concrete contribution to the strength, hence, a weak joint with reduced ductility. Congestion may also lead to limitations on the beam bar sizes relative to the joint dimensions. Experimental and analytical work has shown that the yield strength cannot be developed fully in a stirrup leg adjacent to a hook or a bend [2]. This is because the high compressive stress at the inner face of the bends may cause crushing or splitting of the concrete, resulting in slip before the yielding force can develop.

Steel headed studs have been used extensively for reinforcing thin concrete flat plates against punching shear around the columns [3]. A stud is a straight bar with an anchor head forged or welded onto one or both ends. Stems of double-headed studs are normally made of plain bars without surface deformations (Fig. 1). Bearing of the head against concrete provides superior anchorage. With area of the head equal to 9 to 10 times the stem cross-sectional area, full yielding of the stem can develop, with negligible slip, immediately behind the head [4]. This eliminates the need for the hooks, bends or development length required in conventional reinforcement.

Figure 1. Double headed studs with plain stem.

The stud shear reinforcement has been used in flat slabs, footings, and raft foundations of hundreds of structures around the world. Headed studs have also been proposed for many other applications. Several studies have shown that stud reinforcement provides better confinement and hence enhanced ductility of concrete elements. Tests were done on corbels reinforced with double-headed studs as primary tension reinforcement [5], on I-beams with the studs used as web shear reinforcement [6], and on dapped-end beams with single- and double-headed studs used as shear reinforcement to the dapped-end zones [7]. Tests were also conducted to demonstrate the efficiency of double-headed studs in confining concrete in columns [8] and shear walls [9] under cyclic loading.

The use of headed bars in place of hooked bars for beam flexural reinforcement to ease congestion in exterior and roof corner beam-column joints has been investigated by several researchers. Wallace et al. [10] conducted cyclic loading tests on exterior inter-storey and roof corner beam-column joint subassemblies built with the 90-degree hooked beam flexural bars replaced by straight bars with threaded or friction-welded anchor head at the bar end embedded in the joint. Beam bars of 16, 20, and 25 mm in diameter with a relatively large head-to-bar area ratio (between 4 and 11) were used. Wallace et al. [10] concluded that performance of the specimens with headed bars was as good as that of similar specimens with standard 90-degree hooks. Chun et al. [11] extended the investigation to joints with larger-diameter bars (22, 32, and 36 mm) and a relatively small head-to-bar area ratio. They concluded that a ratio between 3 and 4 is sufficient for effective anchorage of beam bars within exterior beam-column joints. The recommendations of Wallace et al. [10] and Chun et al. [11] to allow the use of headed bars terminating in beam-column joints are adopted by the Joint ACI-ASCE Committee 352 report, "Recommendations for Design of Beam-Column Connections in Monolithic Reinforced Concrete Structures (ACI PRC-352-02)" [12].

Other investigations into the use of headed bars in beam-column joints are available in the literature [13-18]. Chutarat and Aboutaha [13] investigated experimentally the possibility of relocating the plastic hinge in beam-column joints away from the interface with the column by means of double-headed bars placed parallel to the beam bars at top and bottom. Lee et al. [14] tested eccentric beam-column joints with the beams reinforced with screw-deformed bars anchored within the joint using one or two flange nut-like anchorage device. Chun et al. [15] tested thirty exterior beam-column joints without transverse reinforcement to evaluate the anchorage strength of beam bars with different anchorage configurations and embedment lengths.

The ACI PRC-352-02 [12] includes a list of areas in need of further research about beam-column joints. One of these needs is for innovative joint designs that can reduce congestion of reinforcement and use of headed bars in the joints. The research reported herein is an attempt to fulfil this need. It examines the potential and investigates the efficacy of using double-headed studs as shear reinforcement in lieu of conventional closed hoops and crossties in concrete beam-column joints. This paper presents results of an experimental investigation into the behavior of joints reinforced with double-headed studs under quasi-static cyclic loading producing high levels of inelastic deformations similar to those experienced in severe earthquakes. Different arrangements and amounts of studs are investigated. A comparison is made with the behavior of a joint without shear reinforcement and with that of a joint designed according to the ACI 318 Code provisions and reinforced with conventional closed hoops and crossties.

SHEAR STRENGTH PREDICTION MODELS AND CODE PROVISIONS

Two main analytical models, known as the diagonal compression strut mechanism and the truss mechanism, are commonly used to describe the flow of forces in the joint and to determine the amounts of transverse reinforcement required for developing the joint shear capacity [1]. The two models constitute the basic concepts for the design and detailing of beam-column joints by different international standards. A strong agreement exists among provisions of the ACI Code, ACI 318-14 [19], the Canadian Standards, CSA A23.3-14 [20], and the Eurocode 8, EN 1998-1:2004 [21], for the design and detailing of beam-column joints. The three codes assume severe deterioration of bond of the reinforcing bars in the joint, and thus, adopt the diagonal strut mechanism, in which the joint shear capacity is limited by the strength of the strut. Therefore, considerable amounts of transverse reinforcement (closed hoops and crossties) are specified to provide confinement and ensure high strength of the diagonal strut. However, a limit on the shear capacity is specified to avoid brittle compression failure of the strut. The confinement is extended to cover the critical regions in the column and the beam adjacent to the joint.

Both the diagonal strut and the truss mechanisms are incorporated in the New Zealand NZS 3101 Standard [22] based on an assumption that bond of the reinforcing bars in the joint is sufficient for transfer of the shear forces to the joint core. Thus, a significant amount of transverse reinforcement is required to ensure formation of the truss mechanism in the joint.

Many researchers have attempted to introduce analytical models other than the diagonal strut and truss models to better explain the joint behavior and consequently achieve better design. The strut-and-tie model (STM), first introduced by Schlaich et al. [23], presents a more rational approach for explaining the transfer of forces and determining the amount of reinforcement needed in discontinuity regions such as beam-column joints. Hwang and Lee [24] proposed a so-called "*softened*" strut-and-tie (SST) model for evaluation of the shear strength of exterior beam-column joints under cyclic loading. The SST model accounts for the nonlinear constitutive relation and softening of concrete due to cracking. In the SST model, the resultant of the joint vertical and horizontal shear is transmitted through inclined struts, a vertical tie, and a horizontal tie (Fig. 2). The vertical and horizontal ties are represented, respectively, by the column vertical bars and the hoops and crossties in the joint. Proportioning the resultant among the struts and ties is done through distribution factors. The forces in the ties determine the required amount of reinforcement. The compressive stresses resulting on the nodes are checked against the concrete strength "*softened*" by the tensile stresses perpendicular to the struts.

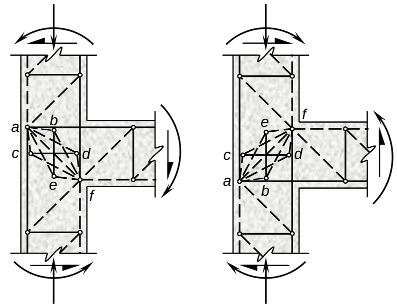

Figure 2. Softened strut-and-tie model [24].

Based on their SST model, Hwang et al. [25] argued that the major function of the joint transverse reinforcement is more in resisting shear than in confining the concrete core. They tested nine exterior beam-column joint specimens reinforced with different amounts and detailing of hoops and crossties to support their argument and show that the ACI Code overestimates the shear strength of exterior beam-column joints.

ACI Code provisions

For seismic design of exterior beam-column joints, the ACI 318-14 [19] Code specifies the following major requirements:

1. Flexural strength ratio: To ensure a strong-column weak-beam design and to produce flexural hinging in the beam rather than the column, the sum of the nominal flexural strengths, $\sum M_{nc}$, of the column sections above and below the joint should not be less than 1.2 times the sum of the nominal flexural strength, $\sum M_{nb}$, of the beam sections at the joint.
2. Joint shear strength: To prevent shear failure of the joint before formation of a hinge in the beam, the design shear force on the joint shall not exceed the code specified limit. The horizontal shear force on the joint, V_{jh}, is estimated as:

$$V_{jh} = T - V_{column} = \alpha\, f_y\, A_s - \frac{M_{nb}}{H} \tag{1}$$

where T, A_s, and f_y, respectively, are the tension force, the cross-sectional area, and the yield strength of the beam reinforcing bars; V_{column} is the shear in the column, and H is the column height. The factor α is a stress multiplier accounting for overstrength and strain hardening of the beam bars; $\alpha = 1.25$ for joints designed for seismic resistance. The beam nominal moment capacity, M_{nb}, in Eq. (1) is calculated based on αf_y. The vertical shear on the joint can be determined from equilibrium.

The joint nominal shear strength, V_n, is specified by ACI 318 as:

$$V_n = \gamma \sqrt{f_c'}\, b_j\, h \tag{2}$$

where f_c' is the compressive strength of concrete; b_j is the joint effective width as defined in Fig. R21.7.4 of ACI 318-14, but not greater than the overall width of the column; and h is the overall depth of column. The factor $\gamma = 1.0$ when f_c' is in MPa for an exterior beam-column joint without transverse beams framing into the joint.

3. Joint confinement: To maintain the shear strength and integrity of the joint after cracking, the codes require adequate horizontal confinement of the joint core. If beams framing into the joint do not provide sufficient confinement, closely spaced transverse reinforcement must be provided within the joint. For rectangular columns, the minimum amount of closed hoops and crossties is specified by ACI 318-14 as:

$$A_{sh} = 0.3\, s\, b_c \frac{f_c'}{f_{yt}} \left(\frac{A_g}{A_{ch}} - 1 \right) \quad \text{but not less than} \quad 0.09\, s\, b_c \frac{f_c'}{f_{yt}} \tag{3}$$

where A_{sh} is the total cross-sectional area of all legs of hoops and crossties within a spacing s measured vertically center-to-center of the hoops; A_g is the gross cross-sectional area of the column; A_{ch} is the cross-sectional area of the column core, measured to the outside edges of the transverse reinforcement that constitute A_{sh}; and f_{yt} is the yield strength of the transverse reinforcement. Equation (3) is to be satisfied in both cross-sectional directions of the rectangular core. For each direction, b_c is the core dimension perpendicular to the hoop legs and crossties that compose A_{sh}.

4. Anchorage of beam bars: To ensure adequate anchorage of the beam bars within the joint, ACI 318-14 requires the use of 90-degree hooked bars with minimum development length, ℓ_{dh}, specified as the largest of $8d_b$, 150 mm, and

$$\ell_{dh} = \frac{f_y}{5.4\sqrt{f_c'}} d_b \quad \text{(mm)} \tag{4}$$

where f_y and d_b, respectively, are the yield strength in MPa and the diameter in mm of the beam bar.

Softened strut-and-tie (SST) model

Figure 2 represents a strut-and-tie model idealization of the joint under reversed loading [24]. From equilibrium, the joint horizontal and vertical shear, V_{jh} and V_{jv}, are given by:

$$V_{jh} = D\cos\theta + F_h + F_v \cot\theta \tag{5}$$

$$V_{jv} = D\sin\theta + F_h \tan\theta + F_v \tag{6}$$

where D is the compression in the diagonal strut, *af*, inclined at an angle θ to the horizontal; F_h and F_v are the tensile forces in the horizontal tie, *cd*, and the vertical tie, *be*, respectively. The shear force, V_{jh}, can be obtained from Eq. (1) and the force V_{jv} from equilibrium. The forces F_h, F_v, and D, respectively, can be expressed as:

$$F_h = R_h V_{jh} \;; \quad F_v = \frac{R_v}{\cot\theta} V_{jh} \;; \quad \text{and} \quad D = \frac{R_d}{\cos\theta} V_{jh} \tag{7}$$

where R_d, R_v, and R_h are distribution factors given by:

$$R_h = \frac{\gamma_h(1-\gamma_v)}{1-\gamma_h\gamma_v} \;; \quad R_v = \frac{\gamma_v(1-\gamma_h)}{1-\gamma_h\gamma_v} \;; \quad \text{and} \quad R_d = \frac{(1-\gamma_h)(1-\gamma_v)}{1-\gamma_h\gamma_v} \tag{8}$$

where
$$\gamma_h = \frac{2\tan\theta - 1}{3} \qquad \text{with } 0 \le \gamma_h \le 1 \tag{9}$$

and
$$\gamma_v = \frac{2\cot\theta - 1}{3} \qquad \text{with } 0 \le \gamma_v \le 1 \tag{10}$$

The forces in the ties are related to the steel strains as follows:

$$F_h = A_{sh} E_s \varepsilon_h \le F_{yh} \tag{11}$$

$$F_v = A_{sv} E_s \varepsilon_v \le F_{yv} \tag{12}$$

where A_s, E_s, ε_s, and F_y, respectively, are the cross-sectional area, modulus of elasticity, strain, and yield strength of steel; subscripts h and v refer to the horizontal and the vertical ties, respectively. The reinforcement areas A_{sh} and A_{sv} can be determined by setting ε_{sh} and ε_{sv} less than or equal to the steel yield strain in Eqs. (11) and (12), respectively.

The maximum compressive stress on the nodal zone, where the forces from struts *af*, *ad*, and *ae* meet at node *a* and from struts *af*, *bf*, and *cf* meet at node *f* (Fig. 2), can be calculated as:

$$\sigma_{d,\max} = \frac{1}{A_{str}} \left[D + \frac{\cos(\theta - \theta_f)}{\cos\theta_f} F_h + \frac{\cos(\theta_s - \theta)}{\sin\theta_s} F_v \right] \tag{13}$$

where θ_ϕ and θ_s, respectively, are the inclinations of the flat struts *ad* and *cf* and the steep struts *ae* and *bf* to the horizontal; $A_{str} = a_s b_s$ is the effective area of the diagonal strut *af*, with a_s and b_s being the strut depth and width, respectively. The depth a_s is given as:

$$a_s = \sqrt{c_b^2 + c_c^2} \tag{14}$$

where c_b and c_c are the depth of compression zone in the beam and the column, respectively. The width b_s of the diagonal strut can be taken equal to the joint effective width as defined in Fig. R18.8.4 of ACI 318-14.

The joint reaches its strength when the maximum stress, $\sigma_{d,\max}$, in the direction of the diagonal strut as calculated from Eq. (13), reaches a value σ_d obtained from a softened stress-strain relationship proposed by Zhang and Hsu [26] as follows:

$$\sigma_d = \xi f_c' \left[2\left(\frac{\varepsilon_d}{\xi\varepsilon_o}\right) - \left(\frac{\varepsilon_d}{\xi\varepsilon_o}\right)^2 \right] \quad \text{for} \quad \frac{\varepsilon_d}{\xi\varepsilon_o} \le 1 \tag{15}$$

where $$\varepsilon_o = -0.002 - 0.001\left(\frac{f_c' - 20}{80}\right) \quad \text{for } 20 \le f_c' \le 100 \text{ MPa} \tag{16}$$

and ξ is a softening coefficient given as:

$$\xi = \frac{5.8}{\sqrt{f_c'}} \frac{1}{\sqrt{1+400\,\varepsilon_r}} \le \frac{0.9}{\sqrt{1+400\,\varepsilon_r}} \tag{17}$$

and ε_r being the principal strain. Hwang and Lee [27] assumed $\varepsilon_r = 0.005$ and proposed an approximation for ξ as:

$$\xi = \frac{3.35}{\sqrt{f_c'}} \le 0.52 \tag{18}$$

EXPERIMENTAL PROGRAM

A total of six full-scale beam-column joint specimens were tested under cyclic loading. Each specimen represented an exterior beam-column joint subassembly isolated at the points of contra-flexure from a typical multi-storey, multi-bay reinforced concrete frame. The concrete dimensions and the beam and column reinforcing details were the same in all the six specimens (Fig. 3). The beam length from the column face was 1.80 m, with a 1.65 m distance to the point of contra-flexure. The column was 3.0 m high, with a 2.75 m distance between the points of contra-flexure. Both the beam and the column had the same cross-section dimensions of 300 mm width and 400 mm depth. The beam was reinforced with 4-20M bars top and bottom. The column was reinforced with 3-20M bars on each side and one intermediate 15M bar on each face. Size 10M closed hoops and stirrups were placed in the column and the beam in accordance with ACI 318-14. The specimens differed only in the reinforcing details of the joint as described below. The design of the specimens was based on concrete compressive strength of 30 MPa and specified yield strength of 400 MPa for reinforcing steel. An axial load producing compressive stress of $0.1\,f_c'$ on the column was used in the design.

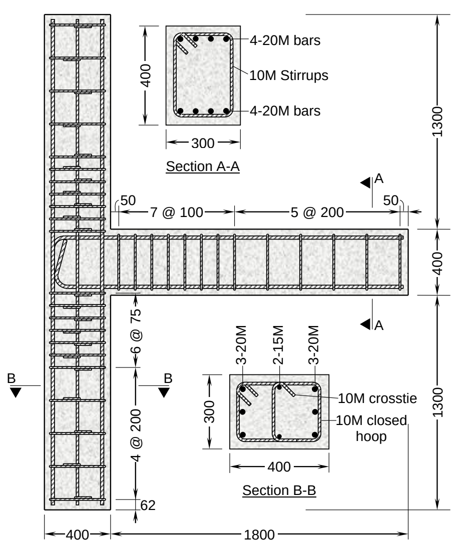

Figure 3. Typical concrete dimensions and reinforcing details of test specimens.

Specimen design and reinforcing details

Specimen CSD was a Control Shear-Deficient specimen designed without any transverse shear reinforcement in the joint. Figure 4a depicts a schematic view of the reinforcing details and the reinforcing cage of joint specimen CSD.

Specimen CCD was a Control Code-Designed specimen representing a joint detailed according to ACI 318-14. The transverse reinforcement in the joint consisted of 4-10M conventional closed hoops and 4-10M crossties spaced vertically at 75 mm center-to-center. The amount was determined from Eq. (3) applied in both the in-plane and out-of-plane directions. The spacing was taken as specified in Clause 18.7.5.3 of ACI 318-14. The crossties were used to tie the intermediate 15M bars in the column and to provide additional confinement in the out-of-plane direction. The joint reinforcing details and the assembled cage are shown in Fig. 4b which clearly shows significant steel congestion in the joint.

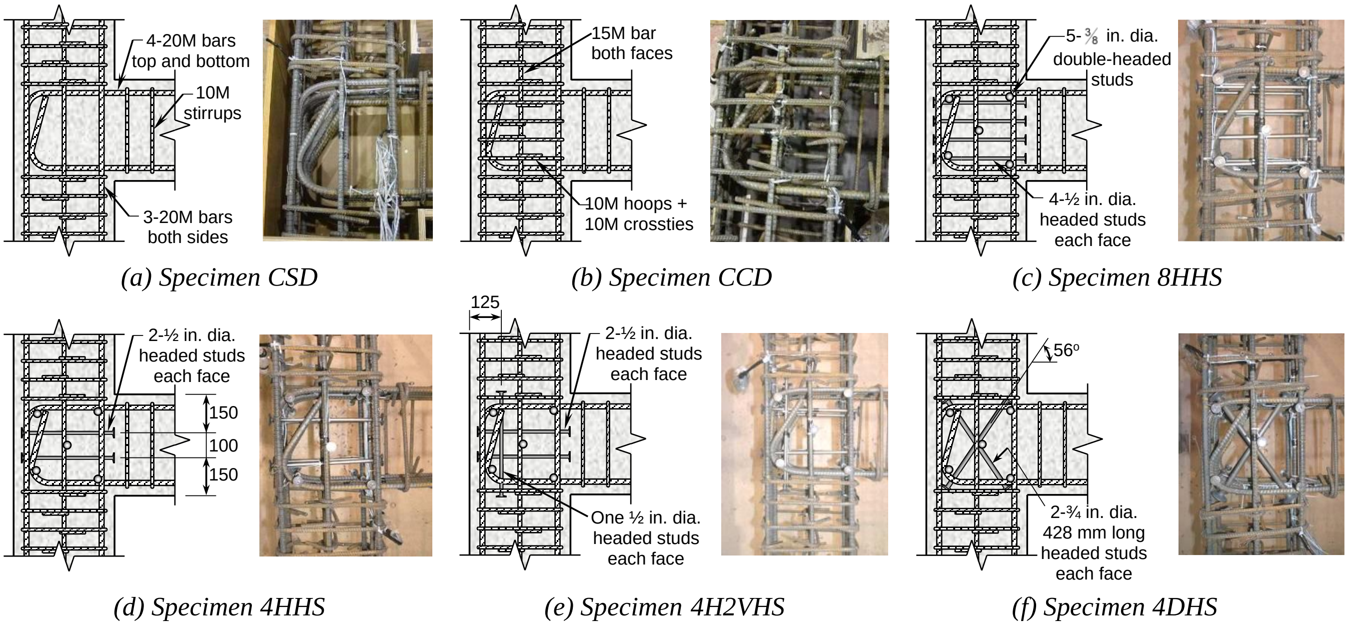

Figure 4. Details of joint reinforcement in the test specimens.

Specimen 8HHS represented a joint where the conventional hoops and crossties in specimen CCD were replaced by horizontal double-headed studs. Eight 12.7 mm dia. studs of 1000 mm^2 total cross-sectional area were used in the in-plane direction (Fig. 4c) replacing the hoop legs in the same direction of specimen CCD. Five 9.5 mm dia. studs were provided in the out-of-plane direction. The cross-sectional area of these studs was close to 30% of the area provided in the out-of-plane direction by the closed hoops and crossties in specimen CCD. This reduction was intended to assess the effect of out-of-plane confinement on the joint performance.

Specimen 4HHS was similar to specimen 8HHS except that the joint and the horizontal in-plane double-headed studs were designed according to the SST model (Fig. 2) of Hwang and Lee [24]. From Eq. (1), the joint horizontal shear, $V_{jh} = 531$ kN. For the joint dimensions of the test specimens, $\theta = 45$ degrees, $\gamma_h = \gamma_v = 0.33$ [Eqs. (9) and (10)], and Eq. (8) gives distribution factors $R_h = R_v = 0.25$, and $R_d = 0.5$. Thus, Eq. (7) gives the forces in the horizontal and vertical ties and the diagonal strut as: $F_h = F_v = 133$ kN and $D = 375$ kN. The minimum yield strength of the headed studs as specified by the manufacturer is 350 MPa. Equation (11) gives the required area of the horizontal tie, $A_{sh} = 380$ mm^2. Four 12.7 mm dia. double-headed studs were used as shown in Fig. 4d to serve as a horizontal tie. The two 15M intermediate bars of the column served as the vertical tie. With $f_y = 400$ MPa, the 2-15M intermediate bars of the column were sufficient to carry the force in the vertical tie. Similar to specimen 8HHS, five 9.5 mm dia. double-headed studs were provided in the out-of-plane direction. The concrete stresses in the nodal zone due to forces in all struts meeting at the node need to be checked against the softened concrete strength. From the joint dimensions, the flat and steep struts are inclined to the horizontal at $\theta_f = 26.5$ degrees and $\theta_s = 63.4$ degrees, respectively. With the effective area of the diagonal strut, $A_{str} = 44{,}045$ mm^2, Eq. (13) gives the nodal compressive stress, $\sigma_{d,\max} = 14.9$ MPa. The softened compressive strength of concrete in the node is $\sigma_d = \xi f_c'$ from Eq. (15). With $\xi = 0.52$ from Eq. (18), $\sigma_d = 15.6$ MPa, which is greater than $\sigma_{d,\max}$.

Specimen 4H2VHS was also designed according to the same SST model as specimen 4HHS except that the vertical tie was provided by two 12.7 mm dia. double-headed studs in addition to the original 2-15M vertical bars in the column. The horizontal tie remained represented by four 12.7 mm dia. double-headed studs as shown in Fig. 4e. Addition of the vertical studs was intended to assess the effect of in-plane confinement in the vertical direction. The vertical studs were placed at 125 mm from the column outer edge. The purpose was to delay and control the diagonal crack that occurs at the column edge triggering joint failure as will be discussed later.

Specimen 4DHS represented a joint reinforced by diagonal double-headed studs according to a strut-and-tie model developed by the authors as shown in Fig. 5. Analysis of the model was performed using the computer program CAST [28]. The forces applied to the joint region and the strut and tie forces resulting from the analysis are shown in Fig. 6. The applied loads $V = 125$ kN, and $T = C = 688$ kN, are equivalent to the capacity of specimen CCD recorded during its test. The reinforcing area needed to carry the 228 kN in the diagonal tie *b-d* was provided by two 19.1 mm dia. double-headed studs in each direction as shown in Fig. 4f. With the total cross-sectional area of the two studs equal to 574 mm^2, the strain in the diagonal tie is equal to 0.0019. As the tie is transverse to the diagonal strut, it can be assumed that the average principal strain, ε_r, in the concrete is equal to the strain in the tie. Thus, Eq. (17) gives a softening coefficient $\xi = 0.68$. The concrete softened strength is then $\sigma_d = \xi f_c' = 20.4$ MPa. The resultant of the forces in the struts meeting at node *a* or *c* is equal to 758 kN giving a maximum stress on the nodal zone $\sigma_{d,\max}$ = 17.3 MPa which is less than σ_d. The joint was also reinforced with five 9.5 mm dia. double-headed studs in the out-of-plane direction. It should be noted that the area provided by these five studs was chosen arbitrarily and was kept constant for all the four specimens 8HHS, 4HHS, 4H2VHS, and 4DHS in order to examine the effects of the layout and the amount of the in-plane double-headed studs on the joint shear strength.

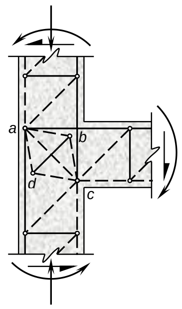

Figure 5. SST model with diagonal ties in the joint.

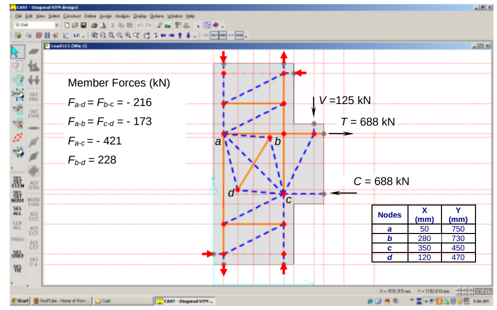

Figure 6. Analysis STM for specimen 4DHS.

Test setup

Figure 7a shows schematically the deformed shape of a typical exterior beam-column joint subassembly isolated at the points of contra-flexure in a multi-storey moment resisting frame subjected to lateral loads. The inter-storey drift angle, θ, is defined as the column relative lateral displacement, δ_{col}, divided by the column height, *H*. The drift angle can also be calculated from the beam-tip vertical displacement, δ_{beam}, that would occur if the beam free body rotation were allowed. For testing a beam-column joint specimen, it is practical to have the column ends pinned with restrained lateral displacement while the beam tip is displaced vertically (Fig. 7b). In this case, the column shear in the specimen, V_{test}, and the corresponding shear in the actual frame, V_{actual}, can be calculated as:

$$V_{test} = \frac{F\left(L/2\right)}{H} \quad \text{and} \quad V_{actual} = V_{test} - \theta\left(\frac{F}{2} + P\right) \tag{19}$$

where *F* is the vertical force acting on the beam tip; *L* is the beam length measured center-to-center of the supporting columns; *H* is the column height; and *P* is the axial load on the column.

Figure 8 is a schematic view of the test setup. A hydraulic jack was used to apply an axial force *P* = 360 kN to the column causing a compressive stress of 10% of the concrete strength. A 250 kN actuator was used to apply a force *F* at the beam tip in a displacement-controlled mode. The column was pinned laterally at its top and bottom to the testing frame. The maximum moment, *M*, on the beam at the column face was equal to $F\,\ell$, with $\ell = 1650$ mm. A roller support was placed under the column, and a spherical seat was transferring the axial force to the column top. Lateral supports were used to restrain the beam from possible twist and lateral deflection.

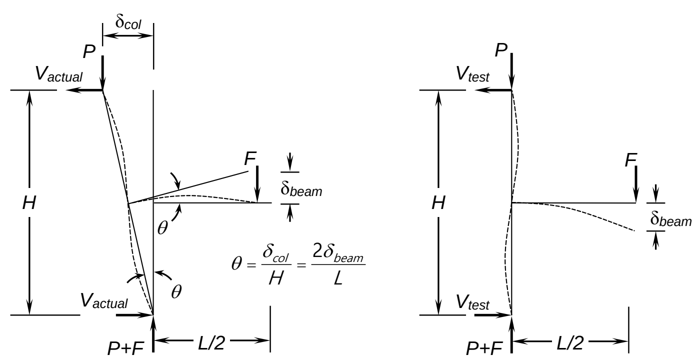

(a) in the idealized structure *(b) in the test specimen*

Figure 7. Inter-storey drift angle.

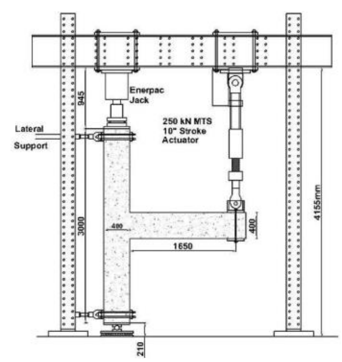

Figure 8. Test setup.

Loading routine

Before application of cyclic loading, an axial load of $0.1 f'_c A_g = 360$ kN was applied to the column and kept constant throughout the test. A quasi-static cyclic load was then applied at the beam tip in a displacement-controlled mode. Quasi-static cyclic loading gives conservative estimate of the strength as the dynamic forces due to earthquakes increase the strain rate and, hence, the strength and stiffness [1]. The loading history consisted of series of three identical displacement cycles. The displacement amplitude was progressively increased from one series to another by a 5 mm increment in each of the upward and downward directions (Fig. 9). The rate of application was 0.25 mm/sec up to 35 mm displacement, after which the rate was increased to 1.0 mm/sec. This loading sequence was intended to produce high levels of inelastic deformations similar to those experienced in severe earthquakes. The displacement amplitudes and loading rates were selected to enable investigating the elastic and inelastic behavior as well as failure of the specimen. The slower loading rate was chosen to enable tracking the formation and propagation of cracking, spalling of the concrete cover, and yielding of the reinforcement. Testing was terminated when reduction of 75 percent of the peak load or a drift ratio of more than 5.5 percent was attained.

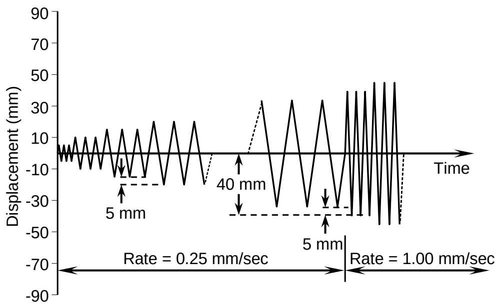

Figure 9. Loading routine.

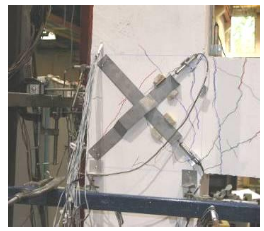

(a) Displacement transducers

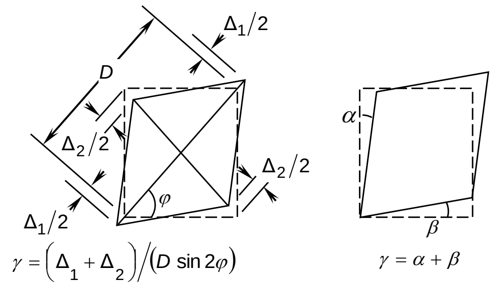

(b) Shear deformation angle

Figure 10. Measurement and calculation of the joint shear deformation angle.

Instrumentation

Two load cells were used to measure the axial load, P, on the column and the vertical load, F, on the beam tip. Displacement transducers and spring potentiometers were used to measure the displacement at various locations. One potentiometer was attached to the bottom of beam tip at the point of application of load F to measure the deflection, δ_{beam}. Displacement transducers were mounted diagonally on the joint to measure the joint shear deformations (Fig. 10a). The shear deformation angle, γ, is calculated directly from the diagonal transducers' readings or from the deformation angles α and β with the vertical and the horizontal directions, respectively (Fig. 10b). To measure the rotation of the plastic hinge in the beam, three displacement transducers were mounted on top and bottom of the beam at the potential location of the hinge, covering a distance of 600 mm from the column face. Electrical resistance strain gauges were used to measure the strain in the joint shear reinforcement and in the beam flexural reinforcing bars at locations near the column face, at mid-width of the joint, and just before the bend at the end of the joint.

EXPERIMENTAL RESULTS AND DISCUSSION

Specimen behaviour

The hysteresis loops describing the load-displacement relationship at the beam-tip are plotted in Fig. 11 for each specimen. The modes of failure of all specimens are shown in Fig. 12.

Specimen CSD: Since this specimen was designed to be shear-deficient without transverse reinforcement in the joint, failure was expected to occur in the joint. The first flexural crack appeared at 5 mm displacement in the beam at the column interface. The first diagonal crack appeared in the joint at 10 mm displacement. Diagonal cracks in the joint reached 0.1 mm width at 15 mm displacement. Yielding of the beam bars was first observed at 35 mm displacement at a 103.5 kN load, and the plastic hinge started to form in the beam initiating degradation of stiffness and increase in the area of the hysteresis loops (Fig. 11a). An ultimate load of 108.9 kN was reached at 55 mm displacement (Fig. 12a). At that load, the joint cracks became unstable, and the load dropped till complete failure of the joint. Failure started with formation of two major diagonal cracks propagating from the centre towards the upper and lower corners of the joint on the column edge. The two cracks passed through the centres of the bends of the beam bars in the direction of high compressive stresses exerted by the bends on the joint concrete core. The cracks continued to propagate parallel to the column reinforcement accompanied by bulging of the joint in both the in-plane (at the column edge) and out-of-plane directions due to lack of confinement of the joint core. Figure 12g shows the specimen at failure.

Specimen CCD: This specimen was expected to fail in the beam. Similar to specimen CSD, the first 5 mm displacement caused a flexural crack to appear in the beam at the interface with the column. At 10 mm displacement, the first diagonal crack appeared at the top corner of the joint, extending from the first flexural crack at the beam-column interface. Yielding of the beam bars was first observed at 30 mm displacement under 105.8 kN load, at which the plastic hinge started to form in the beam. After yielding, stiffness degradation started, accompanied by an increase in the area of hysteresis loops (Fig. 11b). The crack widths kept increasing and the largest crack reached 0.7 mm width at 60 mm displacement. A peak load of 123.8 kN was reached at 90 mm displacement (Fig. 12b), at which the joint cracks stabilized while the beam cracks continued to widen. The load dropped till failure of the beam at the plastic hinge. Figure 12h shows the failure at the plastic hinge. Throughout the test, no yielding was observed in the closed hoops or in the crossties reinforcing the joint. The strain in the closed hoops reached 2100 με in the in-plane direction and 2500 με in the out-of-plane direction. The strain in the crossties reached 1000 με.

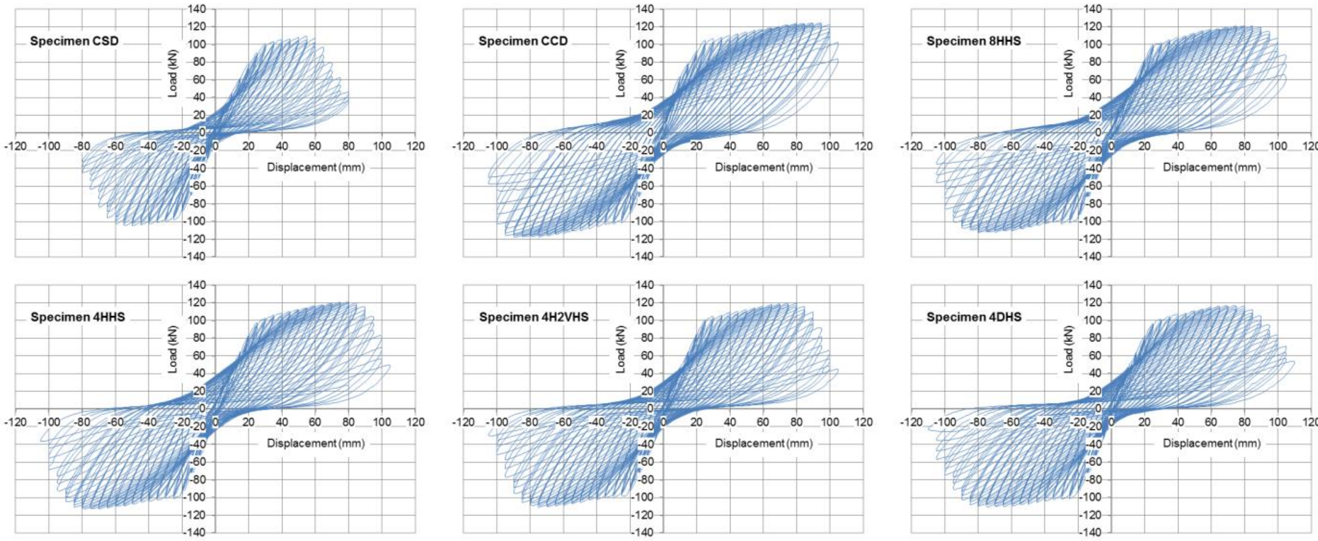

Figure 11. Load-displacement hysteresis loops of the test specimens.

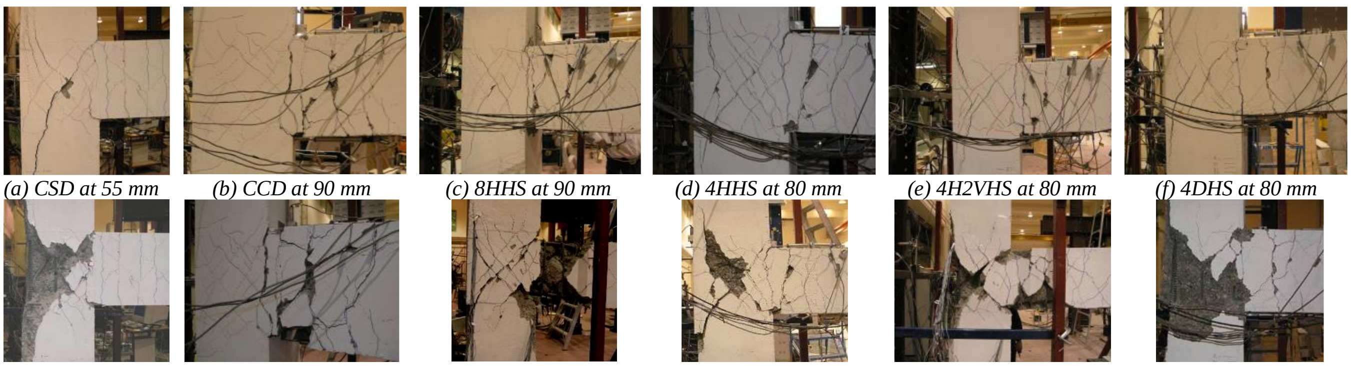

(a) CSD at 55 mm *(b) CCD at 90 mm* *(c) 8HHS at 90 mm* *(d) 4HHS at 80 mm* *(e) 4H2VHS at 80 mm* *(f) 4DHS at 80 mm*

(g) CSD at 80 mm *(h) CCD at 105 mm* *(i) 8HHS at 105 mm* *(j) 4HHS at 105 mm* *(k) 4H2VHS at 105 mm* *(l) 4DHS at 110 mm*

Figure 12. Damage and failure modes of tested joints.

Specimen 8HHS: The first beam crack appeared at the column interface at 5 mm displacement. No cracks appeared in the joint for displacement less than 20 mm. Yielding of the beam bars started at 35 mm displacement and load of 105.4 kN, and the plastic hinge started to form in the beam initiating degradation of stiffness and increase of the area of hysteresis loops (Fig. 11c). At 80 mm displacement the crack width reached 1.0 mm. A peak load of 121.5 kN was reached at 85 mm displacement. No change was observed in the load when the displacement reached 90 mm. Two major diagonal cracks started to appear in the joint at 90 mm displacement (Fig. 12c). However, the cracks in the beam started to widen rapidly, at a much higher rate than the increase of crack width in the joint, and the maximum load continued to decrease till failure occurred in the beam at the plastic hinge at 105 mm displacement. Bulging of the joint occurred only in the out-of-plane direction. No yielding occurred in the shear studs, and the maximum strain recorded was 2500 $\mu\varepsilon$ at 100 mm displacement. The studs perpendicular to the joint yielded at 95 mm displacement, and the maximum strain recorded was 4000 $\mu\varepsilon$. Figure 12i shows failure of the beam at the plastic hinge accompanied by wide cracks at the joint.

Specimen 4HHS: The first beam crack appeared at the column interface at 5 mm displacement. The first joint crack developed at 10 mm displacement and reached 0.24 mm width at 15 mm displacement. Yielding of the beam bars and formation of the plastic hinge started at 35 mm displacement at a load of 105.8 kN (Fig. 11d). A peak load of 120.6 kN was reached at 75 mm displacement and remained constant till 85 mm displacement. The peak load started to drop and the cracks in the joint continued to increase in width while the beam cracks were almost stable until failure took place in the joint. The two major cracks that initiated failure of the joint in specimen CSD were also observed in specimen 4HHS at 80 mm displacement (Fig. 12d). Appearance of these cracks was followed by bulging of the joint indicating an increase in the volumetric strain. Figure 12j shows failure of the specimen at the joint. The two upper horizontal studs yielded at 80 mm displacement and the strain reached 2900 $\mu\varepsilon$ at 100 mm displacement. However, the two lower studs did not yield, and the strain reached 1700 $\mu\varepsilon$. The studs in the out-of-plane direction yielded following extensive cracking that occurred at 80 mm displacement and the strain exceeded 4500 $\mu\varepsilon$.

Specimen 4H2VHS: Figure 11e shows the load-displacement hysteresis loops for this specimen. The first beam crack appeared at the column interface at 5 mm displacement. No joint cracks appeared before 15 mm displacement. Yielding started at 25 mm displacement and 98.05 kN load. A peak load of 120.0 kN was recorded at 75 mm displacement. Cracks in the joint continued to widen while the cracks in the beam were stable. The load capacity decreased till failure occurred in the joint. The two major cracks that initiated the joint failure in specimen CSD started to be seen in specimen 4H2VHS at 80 mm displacement, accompanied by bulging of the joint (Fig. 12e). The specimen was still able to carry a load of 109.7 kN at 90 mm displacement, after which the load continued to drop. The overall behavior was close to that of specimen 4HHS. The addition of the two vertical studs slightly decreased the early cracking but did not enhance the joint performance. However, more beam damage was noticed, and a plastic hinge developed after the joint failure (Fig 12k). The strain levels in the four horizontal in-plane studs were much lower than those of specimen 4HHS (2200 $\mu\varepsilon$). The strain in the two vertical studs changed from tension to compression increasing progressively to yielding shortly before failure. The out-of-plane studs yielded at 80 mm displacement.

Specimen 4DHS: Figure 11f shows the load-displacement hysteresis loops for this specimen. The first beam crack was recorded at the column interface at 5 mm displacement, and the first joint crack was seen at 10 mm displacement and reached 0.06 mm width at 15 mm displacement. Yielding of the beam bars was first observed and the plastic hinge started to form at 35 mm displacement and a 104.4 kN load. A peak load of 115.9 kN was reached at 75 mm displacement and kept almost constant till 80 mm displacement, after which the joint cracks continued to widen while the beam cracks became stable (Fig. 12f). Failure started in the joint by formation of two major cracks similar to those observed in specimens CSD and 4HHS (Fig. 12l). The load dropped till complete failure of the joint. The joint core was not badly damaged. No yielding was observed in the diagonal studs. The maximum strain reached was 2800 $\mu\varepsilon$. The out-of-plane studs yielded at 80 mm displacement and the strain reached 16700 $\mu\varepsilon$.

Storey shear response

Envelopes for the relationship between the actual storey shear and the inter-storey drift angle are plotted and compared in Fig. 13. The figure shows clearly that specimens reinforced with double-headed studs in the joint had much better behavior than the shear-deficient specimen CSD and were close in their behavior to specimen CCD.

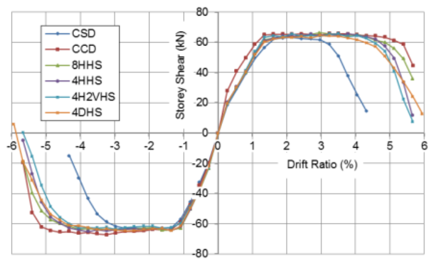

Figure 13. Envelopes of storey shear versus drift ratio.

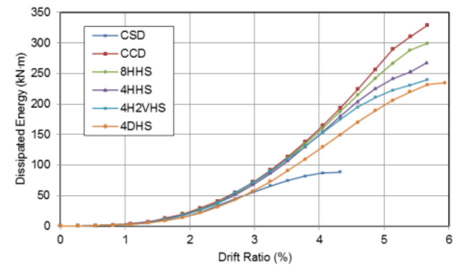

Figure 14. Cumulative dissipated energy versus drift ratio.

Specimen 8HHS exhibited a response very close to that of specimen CCD and failed in a desirable mode at the plastic hinge in the beam. However, the joint of specimen 8HHS experienced more cracks than the joint in specimen CCD. This is attributed to the smaller confinement provided by the five 9.5 mm dia. double-headed studs in the out-of-plane direction in specimen 8HHS in comparison to the confinement provided in specimen CCD by the crossties and the closed hoop legs perpendicular to the joint plane.

Specimens 4HHS and 4H2VHS were designed according to the SST model of Hwang and Lee [24]. The area of the four 12.7 mm dia. studs provided was enough to carry the force in the horizontal tie, and the concrete was checked against the softened strength calculated using the simplified Eq. (18). In the test, the tie did not experience strain levels higher than what was predicted. However, the joint failed by crushing of concrete at a load close to the joint strength. This is attributed again to the lack of sufficient confinement. The SST model does not consider the effect of confinement in the out-of-plane direction. The test results used by Hwang and Lee [24] to verify the SST model were for specimens reinforced with crossties and closed hoops with reinforcing area sufficient to provide good confinement of the joint in the out-of-plane direction. This underlines the importance of out-of-plane confinement of the joint.

The amount of shear reinforcement provided in the joint of specimen 8HHS is twice the amount provided in the joint of specimen 4HHS. However, at almost the same peak load, the steel strain levels were high and of comparable magnitude in both joints. This indicates that the stud shear reinforcement in specimen 8HHS carried a higher force than that in specimen 4HHS. The increase in the force is attributed to the better in-plane confinement provided by the eight headed studs in specimen 8HHS. This proves that, contrary to the conclusions of Hwang et al. [25], the transverse reinforcement in a beam-column joint is needed not only to contribute to the joint shear resistance, but also to provide confinement to the joint concrete core and compression strut. Specimen 4H2VHS had a response close to 4HHS. The vertical Studs did not contribute effectively to the joint behavior especially at high deformation levels. This may be attributed to the fact that with cracking and softening, the concrete in the joint core started to transfer a part of the column axial compressive stresses to the vertical studs. This explains the compressive strains measured at the vertical studs after severe concrete cracking.

Specimen 4DHS exhibited the least desirable behavior of the four specimens reinforced with studs. As the diagonal studs were placed in the direction of the principal tensile stresses, they fulfilled their role as ties and experienced strains well below the yield strain. However, their effect in confining the compression struts was not great. The nodal zones at the beam bar bends, which had the highest compressive stresses and accompanying perpendicular principal tensile stresses, were not fully affected by the compression cones of the stud heads. This again indicates the importance of the confinement to the joint core.

Cumulative energy dissipation

The ability to dissipate energy is the most important factor in seismic design since the higher the ability of the structure to dissipate energy the higher its chances of surviving an earthquake. The energy dissipated in each load cycle is defined by the area enclosed by the hysteresis loop in the load-displacement diagram. The cumulative dissipated energy is the sum of the energy dissipated in the hysteresis loops. The cumulative dissipated energy for each of the five specimens at different displacement levels is presented in Fig. 14. As can be seen, specimen CCD had the highest energy dissipation. The total energy dissipated by specimens 8HHS, 4HHS, 4H2VHS and 4DHS was, respectively, about 90, 81, 77 and 70 percent of that of CCD. Naturally, specimen CSD had the lowest energy dissipation due to lack of shear reinforcement and confinement in the joint.

Joint contribution to the storey drift angle

The joint contribution, θ_j, to the storey drift angle, θ, (Fig. 7) can be calculated from the following equation [29]:

$$\theta_j = \gamma\left(1 - \frac{h_c}{L} - \frac{h_b}{H}\right) \tag{20}$$

where γ is the joint shear deformation angle (see Fig. 10b); h_b and h_c are the beam and column cross-section depth, respectively.

The joint contribution is expressed as percentage of the total drift angle and presented in Fig. 15 for all specimens. As expected, the joint of specimen CSD had the largest contribution due to its large deformations. In specimen CSD, the joint contribution increased from zero to a maximum of 29.6 percent at a drift angle of 0.0162 radians, corresponding to the start of yielding of the beam bars at 35 mm displacement. Because of the increase in the beam deformations after yielding, the joint contribution decreased to 21.6 percent at a drift angle of 0.0324 radians, which was reached at the peak load sustained by the specimen at the beam tip. Because of the extensive joint cracking that followed the peak load, the joint contribution increased rapidly till failure.

The joint contribution in specimen CCD remained practically constant after reaching 10 percent at yielding of the beam bars. Before reaching the peak load, the joint contribution in specimens 8HHS, 4HHS and 4H2VHS was smaller than that in specimen CCD and ranged from 3 to 8 percent, indicating higher stiffness of the joint. Due to excessive cracking after the peak load, the joint contribution increased slightly in specimen 8HHS and dramatically in specimens 4HHS and 4H2VHS.

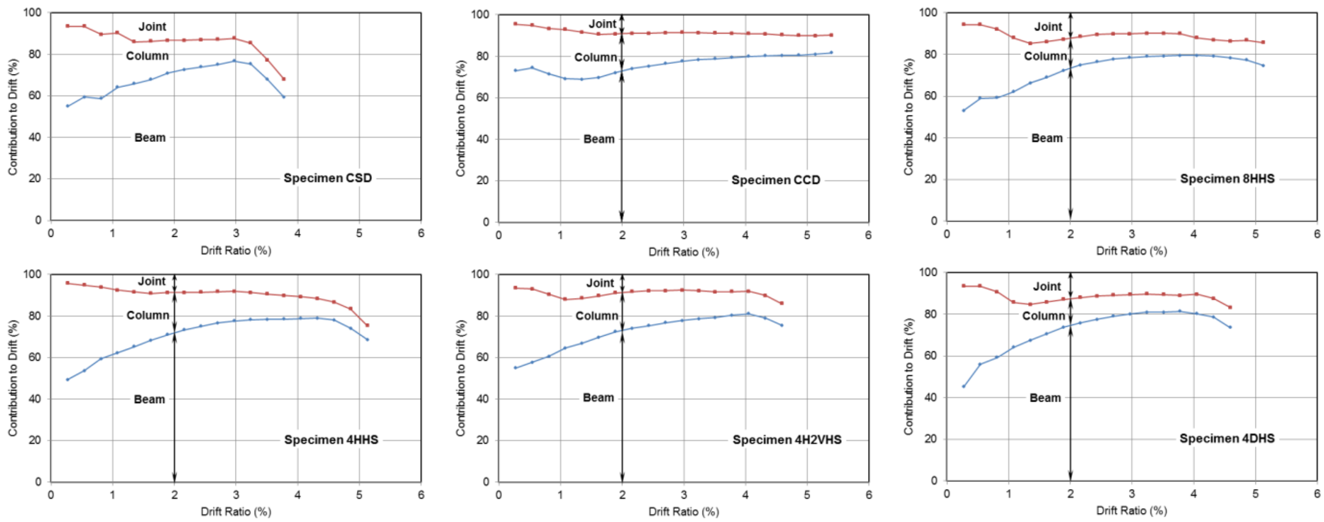

Figure 15. Member contribution to drift ratio.

The joint contribution in specimen 4DHS was close to that of CSD at small drift angles. This shows that the diagonal studs were still not in effect. After early cracking of the joint, the studs became effective and played their role as ties, hence controlled the crack width. Consequently, the joint contribution decreased and became close to that of CCD for drift angles between 0.02 and 0.04 radians. For drift angle larger than 0.04 radians, the lack of confinement to the joint core induced larger cracks and crushing started to take place causing an increase in the joint contribution till failure. The joint in specimen 4DHS had the largest contribution at large drift angles.

These results are consistent with those of the cumulative energy dissipation shown in Fig. 14, since the larger the joint deformation, the more the pinching in the hysteresis loops, and hence, the smaller the enclosed area in each loop.

Joint shear stress versus joint deformation angle

The joint shear stress, Eq. (1) divided by column gross cross-sectional area, versus the joint deformation angle, calculated as per Fig. 10b, in all specimens is compared in Fig. 16. As can be seen, specimen CSD had the least shear strength as it failed at 4.21 MPa and the maximum recorded shear deformation angle before joint failure was 0.016 radians. Specimen CCD had a maximum recorded shear stress of 4.77 MPa at the onset of beam failure and the maximum joint deformation at beam failure was 0.007 radians. In all the joints reinforced with studs, prior to joint cracking, the studs were not in full effect yet and the joint shear stiffness was closer to that of CSD. After cracking, the studs were in full effect and the joint stiffness increased and became closer to that of CCD till the initiation of failure. Specimen 8HHS had a maximum shear stress of 4.68 MPa and maximum recorded deformation of 0.01 radians at beam failure which was higher than that of CCD. Specimen 4HHS had shear strength of 4.66 MPa when the joint failure started and the maximum recorded deformation was 0.017 radians. The joint strength for specimen 4H2VHS was 4.64 MPa which was almost equal to that of 4HHS and the maximum recorded deformation was 0.009 radians. Specimen 4DHS had a joint strength of 4.47 MPa and a maximum recorded joint deformation of 0.008 radians.

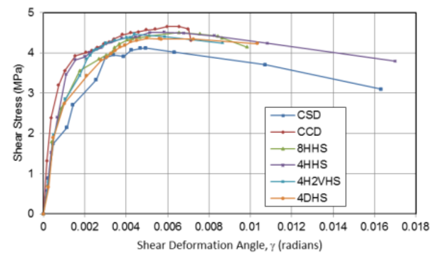

Figure 16. Joint shear stress versus deformation angle.

CONCLUSIONS

Use of double-headed studs is a viable option for shear reinforcing of exterior beam-column joints. The test specimens reinforced with shear studs in the joint achieved considerable enhancement in their behavior under cyclic loads in comparison to a shear-deficient joint and exhibited a performance close to that of a joint reinforced with closed hoops and crossties according to the code. Further studies are in progress to improve detailing of the joint reinforcement with studs to achieve a desirable mode of failure. The following are important conclusions drawn from the present research:

1. The transverse reinforcement in the joint is important for both the shear resistance and confinement.
2. A strut-and-tie design model is proposed with diagonal ties within the joint. The model is not possible to develop without the use of double headed studs.
3. Design according to the softened strut-and-tie model or the proposed model with diagonal ties should consider the need for out-of-plane confinement.
4. Use of double-headed studs as shear reinforcement reduces congestion in the joint considerably and makes assemblage of the cage much easier.
5. Replacing conventional closed hoops and crossties in a code designed joint by horizontal studs of equivalent reinforcing area is effective and leads to a competitive behavior of the joint. However, sufficient out-of-plane confinement is necessary to control excessive joint cracking.
6. The proposed use of studs as vertical ties was not effective in enhancing the joint performance.
7. The proposed diagonal stud arrangement performs well as ties but is not sufficient for confining the joint nodal zones.

ACKNOWLEDGMENTS

This research was financially supported by the Natural Sciences and Engineering Research Council of Canada (NSERC). This support is gratefully acknowledged. The authors also wish to express their gratitude to Decon Canada for donation of the headed studs.

REFERENCES

[1] Paulay, T. and Priestley, M.J.N. (1992). *Seismic Design of Reinforced Concrete and Masonry Buildings*. John Wiley & Sons, New York, USA, 766 pp.

[2] Leonhardt, F. and Walther, R. (1965). "Geschweisste Bewehrungmatten a/s Buegelbewehrung, Schubversuche an Plattenbalken und Verankerungsversuche (Welded Wire Mesh Substitute of Stirrups: Shear Tests on T-Beams and Tests on Anchorage)." *Die Bautechnik*, 42(10), 3-15.

[3] Dilger, W.H. and Ghali, A. (1981). "Shear Reinforcement for Concrete Slabs." *ASCE Journal of the Structural Division*, 107(12), 2403-2420.

[4] Ghali, A., and Dilger, W.H. (1998). "Anchoring with Double-Head Studs." *Concrete International*, 20(11), 21-24.

[5] Birkle, G., Dilger, W.H., Ghali, A., and Schäfer, K. (2001). "Doppelkopfstäbe in Konsolen – Laborversuche und Bemessung (Double-Head Studs in Corbels – Experimental Study and Analysis)." *Beton- und Stahlbetonbau*, 96(2), 82-89 (in German).

[6] Gayed, R.B. and Ghali, A. (2004). "Double-Head Studs as Shear Reinforcement in Concrete I-Beams." *ACI Structural Journal*, 101(4), 550-557.

[7] Herzinger, R. and El-Badry, M. (2007). "Alternative Reinforcing Details in Dapped Ends of Precast Concrete Bridge Girders: Experimental Investigation." *Transportation Research Record*, *TRR*, Journal of the Transportation Research Board, TRB, No. 2028, 111-121.

[8] Youakim, S.A., and Ghali, A. (2002). "Ductility of Concrete Columns with Double-Head Studs." *ACI Structural Journal*, 99(4), 480-487.

[9] Mobeen, S.S., Elwi, A.E., and Ghali, A. (2005). "Double-Headed Studs in Shear Walls." *Concrete International*, 27(3), 59-63.

[10] Wallace, J.W., McConnel, S.W., Gupta, P., and Cote, P.A. (1998). "Use of Headed Reinforcement in Beam-Column Joints Subjected to Earthquake Loads." *ACI Structural Journal*, 95(5), 590-606.

[11] Chun, S.-C., Lee, S.-H., Kang, T.H.-K., Oh, B., and Wallace, J.W. (2007). "Mechanical Anchorage in Exterior Beam-Column Joints Subjected to Cyclic Loading." *ACI Structural Journal*, 104(1), 102-112.

[12] Joint ACI-ASCE Committee 352. (2002). *Recommendations for Design of Beam-Column Connections in Monolithic Reinforced Concrete Structures* (ACI PRC-352-02). American Concrete Institute, Farmington Hills, MI, (Reapproved 2010).

[13] Chutarat, N. and Aboutaha, R.S. (2003). "Cyclic Response of Exterior Reinforced Concrete Beam-Column Joints Reinforced with Headed Bars – Experimental Investigation." *ACI Structural Journal*, 100(2), 259-264.

[14] Lee, H.-J. and Yu, S.-Y. (2009). "Cyclic Response of Exterior Beam-Column Joints with Different Anchorage Methods." *ACI Structural Journal*, 106(3), 102-112.

[15] Chun, S.-C., Oh, B., Lee, S.-H., and Naito, C.J. (2009). "Anchorage Strength and Behavior of Headed Bars in Exterior Beam-Column Joints." *ACI Structural Journal*, 106(5), 579-590.

[16] Kang, T.H.-K., Shin, M., Mitra, N., and Bonacci, J.F. (2009). "Seismic Design of Reinforced Concrete Beam-Column Joints with Headed Bars." *ACI Structural Journal*, 106(6), 868-877.

[17] Kang, T.H.-K., Ha, S.-S., and Choi, D.-U. (2010). "Bar Pullout Tests and Seismic Tests of Small-Headed Bars in Beam-Column Joints." *ACI Structural Journal*, 107(1), 32-42.

[18] Hong, S.-G., Chun, S.-C., Lee, S.-H., and Oh, B. (2007). "Strut-and-Tie Model for Development of Headed Bars in Exterior Beam-Column Joint." *ACI Structural Journal*, 104(5), 590-600.

[19] ACI Committee 318. (2014). *Building Code Requirements for Structural Concrete and Commentary* (ACI CODE-318-14). American Concrete Institute, Farmington Hills, MI.

[20] CSA Standards A23.3-14. (2014). *Design of Concrete Structures*. Canadian Standards Association, Rexdale, Ontario, Canada.

[21] Eurocode 8: *Design of Structures for Earthquake Resistance, Part1: General rules, Seismic Actions, and Rules of Buildings*. EN 1998-1:2004, European Committee for Standardization.

[22] NZS 3101:2006, *Concrete Structures Standard, NZS 3101: Part 1, Commentary, NZS 3101: Part 2*. Standards Association of New Zealand, Wellington.

[23] Schlaich, J., Schäfer, K., and Jennewein, M. (1987). "Toward a Consistent Design of Structural Concrete." *PCI Journal*, 32(3), 74-150.

[24] Hwang, S.-J., and Lee, H.-J. (1999). "Analytical Model for Predicting Shear Strengths of Exterior Reinforced Concrete Beam-Column Joints for Seismic Resistance." *ACI Structural Journal*, 96(5), 846-857.

[25] Hwang, S.-J., Lee, H.-J., Liao, T.-F., Wang, K.-C., and Tsai, H.-H. (2005). "Role of Hoops on Shear Strength of Reinforced Concrete Beam-Column Joints." *ACI Structural Journal*, 102(3), 445-453.

[26] Zhang, L.X.B., and Hsu, T.T.C. (1998). "Behavior and analysis of 100 MPa Concrete Membrane Elements." *ASCE Journal of Structural Engineering*, 124(1), 24-34.

[27] Hwang, S.-J., and Lee, H.-J. (2002). "Strength Prediction for Discontinuity Regions by Softened Strut-and-Tie Model." *ASCE Journal of Structural Engineering*, 128(12), 1519-1526.

[28] Tjhin, T.N. and Kuchma, D.A. (2002). "Computer-Based Tools for Design by Strut-and-Tie Method: Advances and Challenges." *ACI Structural Journal*, 99(5), 586-594.

[29] Alcocer, S. and Jirsa, J.O. (1993). "Strength of Reinforced Concrete Frame Connections Rehabilitated by Jacketing." *ACI Structural Journal*, 90(3), 249-261.